TOWARDS NOVEL HYBRID BIOMASS, COAL, AND NATURAL GAS TO LIQUID SYSTEMS: PROCESS SYNTHESIS, GLOBAL OPTIMIZATION, AND SUPPLY CHAIN APPROACHES

Josephine A. Elia, Richard C. Baliban, & Christodoulos A. Floudas
Department of Chemical and Biological Engineering
Princeton University
Princeton, NJ 08544

Abstract

A novel framework has been developed using hybrid feedstocks and a thermochemical based process superstructure that considers various process alternatives to convert coal, biomass, and natural gas to liquid (CBGTL) transportation fuels. Using binary variables to model process decisions and constraints to model proper unit operations, a mixed-integer non-linear optimization model was developed to determine the topology of the CBGTL refinery that produced the lowest cost fuels. The model includes a simultaneous heat, power, and water integration to directly incorporate the tradeoffs between electricity recovery and wastewater treatment in the objective function. A branch-and-bound global optimization framework was developed using piecewise linear underestimators for the nonconvex terms to provide tight relaxations when calculating the lower bound. Based on the local solutions of the process synthesis model for the stand-alone plant design, an energy supply chain optimization problem was formulated to fulfill the transportation fuel demands for the United States with 50% emissions reduction. Results suggest that alternative fuels from domestically available resources can be produced in an economically competitive manner with improved environmental performance compared to petroleum-based fuels.

Keywords

Hybrid Energy Systems, Fischer-Tropsch Liquids, Mixed-Integer Nonlinear Optimization, Biofuels

Introduction

The challenges to reduce dependence on petroleum as energy sources, coupled with efforts to reduce greenhouse gas (GHG) emissions, are exigent problems faced by the US transportation sector. Several studies have been done to explore alternative, non-petroleum based processes to produce liquid fuels that include the production of Fischer-Tropsch (FT) liquids from biomass, coal, and natural gas (Bechtel, 1998; Kreutz et al., 2008, Larson et al., 2009; Vliet et al., 2009; Baliban et al., 2010; Elia et al., 2010) using a synthesis gas (syngas) intermediate. These energy processes have emerged as viable options to address the given challenges due to their capabilities to produce liquid fuels via domestically available sources of carbon-based energy. A common feature of FT-based processes, however, is the large CO_2 amount emitted from the system. Incorporating biomass in fuel production can help reduce GHG emissions due to the carbon uptake from the atmosphere during biomass growth and cultivation, although its amount is limited by the available land area for biomass. Hybrid processes utilizing coal, biomass, and natural gas can take advantage of the benefits of each raw material to yield processes that can be economically competitive with petroleum-based fuels and have reduced GHG emissions.

A novel hybrid energy process was developed where CO_2 is recycled in a closed-loop system using the reverse water-gas-shift reaction, allowing for a conversion rate of up to 100% for the feedstock-carbon to liquid products

(Baliban et al., 2010; Elia et al., 2010, Baliban et al., 2011; Elia et al., 2011). The process utilizes coal, biomass, and natural gas as feedstocks to produce gasoline, diesel, and kerosene (i.e., coal, biomass, and natural gas to liquid (CBGTL) process) in ratios consistent with the US demand. A superstructure detailing a wide array of process topologies was postulated (Baliban et al., 2011) and a mixed-integer nonlinear optimization (MINLP) model was developed to examine the economic trade-offs between each topology and chose the solution with the best economic value. The model for process synthesis was enhanced by including a simultaneous heat and power integration and a series of heat engines that can convert waste heat to energy.

The optimization model for process synthesis with simultaneous heat and power integration defines a nonlinear, nonconvex landscape where high-quality solutions are obtained by finding several locally optimal points from different initial conditions. To obtain a mathematical guarantee of how close the objective value of each solution is to the best possible value, a global optimization branch-and-bound framework is presented. The framework uses piecewise-linear underestimation of bilinear terms and concave cost functions using a logarithmic partitioning scheme for the bilinear terms and a linear scheme for the concave functions. The framework was tested using two case studies. Each case study will have a 50% reduction in GHG emissions from petroleum-based processes.

The potential of the CBGTL process to fulfill US demands is further investigated in an energy supply chain problem to identify a network of CBGTL plants that will produce fuels for the entire country. A mixed integer linear optimization (MILP) model is formulated that provides the optimal locations of the new plants, with a key focus of minimizing the total network cost of fuel production. Factors affecting the optimal locations include the locations and amounts of feedstock sources, the locations and amounts of demands, and the available infrastructure to transport the various commodities, which are extracted from government based databases and serve as input parameters to the mathematical model. The following subsections present the overview of the work, starting from the design of the CBGTL process to the energy supply chain study for the process.

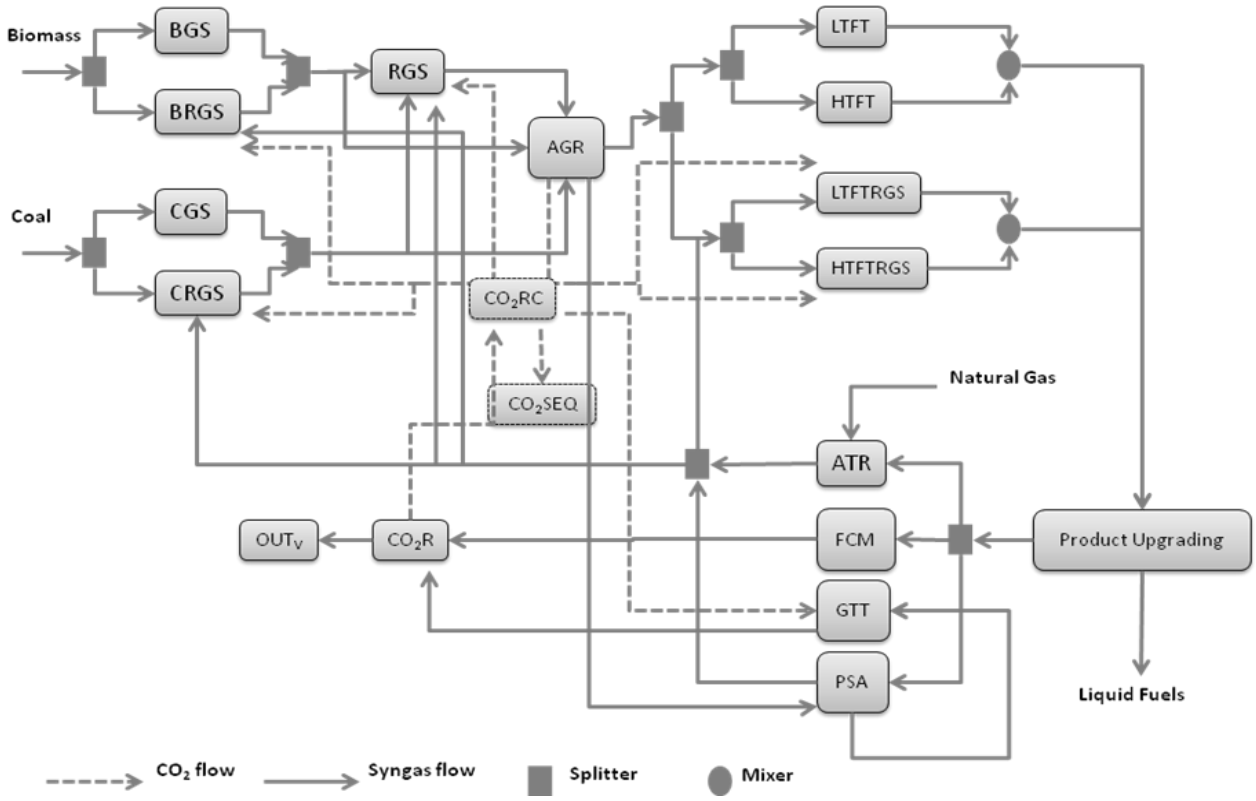

Figure 1. CBGTL Superstructure

Process Synthesis with Simultaneous Heat and Power Integration

CBGTL Conceptual Design

The CBGTL superstructure is shown in Figure 1 and is designed to co-feed a carbon source such as biomass, coal, or natural gas and produce gasoline, diesel, and kerosene transportation fuels. Co-feeding of biomass and coal to the process is done through distinct gasification trains. The biomass and coal gasifiers can either operate with only a solid feedstock input (BGS and CGS) or in tandem with additional vapor phase fuel inputs from elsewhere in the refinery (BRGS and CRGS). The syngas is split and sent directly to the gas cleanup area or to a dedicated reverse water-gas-shift (RGS) unit to consume the CO_2 with H_2 (Agrawal et al., 2007). The gas cleanup area initially consists of an HCl stripper, a COS-HCN hydrolyzer, a wastewater knockout, and a Rectisol acid gas recovery (AGR) unit. The (AGR) unit will provide a clean syngas stream, a pure CO_2 stream, and an acid gas stream. The acid gases are sent to a Claus recovery system to extract elemental sulfur and the CO_2 is either recycled to the CBGTL refinery or sequestered. The acid gas wastewater knockout and all other wastewater streams are sent to a sour stripper column to remove the entrained sour gas from the water.

To produce gasoline, diesel, and kerosene products according to the United States mass demand ratio, two Fischer-Tropsch (FT) reactors are used that operate at different temperatures. Each FT reactor may operate using a cobalt (LTFT and HTFT) or iron based catalyst (LTFTRGS and HTFTRGS) to prevent or facilitate the reverse water-gas-shift (rWGS) reaction. Fuel quality products are obtained by treating the FT effluents in a detailed upgrading section (Bechtel, 1998). The offgas from various upgrading units are split to (i) an auto thermal reactor (ATR), (ii) a combustion (FCM) unit, (iii) a gas turbine (GT) engine, and (iv) a (PSA) unit. The fraction to the combustion unit is determined to satisfy the fuel requirement of the plant. Note that the (ATR) unit is where the natural gas feedstock is introduced into the process. CO_2 is recovered (CO_2R) from the (FCM) unit and the (GTT) and mixed with the CO_2 from the (AGR) unit where it can be pressurized for sequestration (CO_2SEQ) or recycled back to a process unit (i.e., BRGS, CRGS, RGS, LTFTRGS, HTFTRGS) to react with H_2 via the rWGS reaction. The effluent from the (ATR) is split to (i) the solid/vapor fuel gasifiers, (ii) the (RGS) unit, or (iii) the iron-based FT units. The offgas from the (PSA) unit is split and sent to (i) the gas turbine, (ii) the solid/vapor-fueled gasifiers, or (iii) the iron-based FT units. H_2 can be provided by pressure-swing absorption (PSA) or through electrolysis of water (EYZ), and O_2 can be produced by an air separation unit (ASU) or by the (EYZ) unit. Electricity for the process units can be provided from a gas turbine (GT) or from steam turbines in the simultaneous heat exchange and power recovery network. Process wastewater is treated in a sour stripper and mixed with input freshwater where it is used as the (EYZ) feed or heated to form steam and split to various process units.

Economic Assumptions

The production of the refinery is 50,000 barrels per day operating with a capacity of 330 days/year. The investment costs of all process units are estimated from several literature sources. The cost of the switchgrass is \$139.97/dry metric ton, the Illinois #6 coal is \$51.57/dry ton, and the natural gas is \$5.37/standard cubic feet. The cost of electricity is assumed to be \$0.07/kWhr and the cost of CO2 sequestration is \$20/metric ton. All costs are expressed in 2009 \$ using the GDP deflator index.

Computational Results – Optimal Process Topology

As an illustrative example, the investigation of the optimal thermochemical topology for the CBGTL refinery was conducted using two case studies that focused on a 50% or 95% conversion of the feedstock carbon to liquid fuels and a 50% reduction in the greenhouse gas emissions from petroleum-based processes. To locate a high-quality local solution, a multi-start initialization technique is used. As a representative example, the topological results of the 50% conversion case are outlined below. The feedstock carbon from coal accounts for 28.2% of the total carbon input into the system. Biomass and natural gas feedstock each account for 57.0% and 14.2%, respectively, and the rest of the carbon (0.6%) comes from the butane input into the C_4 isomerizer. 49.2% of the input carbon ends up being vented into the atmosphere, a small portion is output as byproduct propane (0.8%), and the balance is output as the main liquid products. No CO_2 sequestration was utilized in this case study.

The biomass gasifier (BRGS) operates at 1000 °C and the coal gasifier (CRGS) at 1200 °C. A dedicated (RGS) unit is not utilized, so the syngas directly enters the cleaning section. 12.8% of the clean syngas stream goes to the (WGS) unit and subsequently fed to the (PSA) unit for H_2 production. The rest of the clean syngas is compressed and split to the iron-based low and high-temperature FT reactors (LTFTRGS and HTFTRGS). The H_2 is sent to the FT reactors to accommodate the rWGS reaction and the various units in the product upgrading section. 71.0% of the light gases from the product upgrading section are reformed in the (ATR) unit, which operates at 700 °C, and the balance is combusted in the fuel combustor (FCM) for plant fuel requirement. 83.6% of the (ATR) effluent is recycled to the (CRGS) unit and the balance to the (BRGS) unit. The recovered CO_2 is entirely sequestered except for a small portion which is used as a carrier gas for the gasifiers. The required O_2 is produced entirely by the (ASU) and sent to the gasifiers, the (ATR) unit, and the Claus combustor.

Computational Results – Overall Liquid Fuels Cost

The costs of liquid fuels production (2009 $) are shown for each case study in Table 1. The overall cost is as a fuels cost in $/GJ of lower-heating value and as a break-even oil price (BEOP) in $/bbl. The BEOP represents the cost of crude oil for which the CBGTL refinery becomes competitive with petroleum-based fuels production and is calculated using the refiner's margin for gasoline, diesel, and kerosene. The BEOP for 50% conversion is $62.50/bbl while that for 95% conversion is $152.90/bbl. The cost increase of $90.40/bbl is clearly visible in the increased electricity cost from the electrolyzers (-$0.36/GJ vs. $19.67/GJ). In fact, for the 50% case, some electricity is generated as a byproduct which may be sold to the grid. The increase in investment cost for the 95% case is due to the large capital required for the electrolyzers. The 95% case does bring about a substantial decrease in the cost of the feedstocks. The coal cost decreases by $1.58/GJ, the biomass by $2.69/GJ, and the natural gas by $0.80/GJ. This corresponds to a total feedstock cost reduction of $5.06/GJ (47.8%). Note that the electricity cost for the 95% case represents 67.5% of the overall cost. If electricity could be available at $0.03/kWhr, then the cost of liquid fuels production would decrease by 38.4% to $93.88/bbl.

Table 1. Breakdown of the overall liquid fuels cost (2009 $/GJ) using a high-quality local solution.

Cost Contribution ($/GJ)	Case Study	
	50% Conv.	95% Conv.
Coal	$3.67	$2.09
Biomass	$5.21	$2.52
Natural Gas	$1.70	$0.90
Butane	$0.54	$0.68
Water	$0.02	$0.03
CO_2 Sequestration	$0.00	$0.00
Investment	$3.05	$3.86
Electricity	-$0.36	$19.67
Propane	-$0.54	-$0.64
Total ($/GJ)	$13.29	$29.12
Total ($/bbl)	$62.50	$152.90

Global Optimization Branch-and-Bound Framework

Origin of Nonlinear Terms

The nonconvex bilinear terms within the mathematical model arise from the multiplication of two positive, continuous variables. These terms are found when a stream composition must be specified, a stream with unknown composition must be split, or a detailed chemical equilibrium must be enforced (Baliban et al., 2010). For phase equilibrium, the appropriate constraint is modeled using the formula $y = K \cdot x$ where y is the composition of the vapor phase, x is the composition of the liquid phase, and K is the equilibrium constant. For all species s flowing from unit u to unit u', the set of composition variables, x^S, that must be specified is termed S_{Fl}. The composition variables are then defined using Eq. 1 where N^s is the species molar flow rate and N^T is the total molar flow rate.

$$N^T_{u,u'} \cdot x^S_{u,u',s} = N^S_{u,u',s} \qquad \forall (u,u',s) \in S_{Fl} \tag{1}$$

The CBGTL process contains four units which enforce phase equilibrium, yielding a total of 92 bilinear terms.

Proper operation of the splitter units requires the composition of the outlet streams to be equal to that of the inlet stream. This may be accomplished using split fractions, $sp_{u,u'}$, for the percentage of flow from the inlet stream, (u_I,u), to each outlet stream (u,u') and enforcing the set of species flow rates (S_{Sp}) using Eq. 2.

$$N^S_{u_I,u,s} \cdot sp_{u,u'} = N^S_{u,u',s} \qquad \forall (u,u',s) \in S_{Sp} \tag{2}$$

The thirteen splitter units within the model produce a total of 164 bilinear terms.

The remaining bilinear terms exist due to the chemical equilibrium that must be enforced by the water-gas-shift reaction and the steam reforming reactions within the auto-thermal reactor. The water-gas-shift equilibrium is defined in Eq. 3 for the syngas species in stream (u,u') using the equilibrium constant, K^{WG}, which is defined by the selection of one of a discrete set of temperature values for the equilibrium unit u''. Equation 3 contains one bilinear term and one trilinear term for each stream, though this equation can be reformulated into two inequalities which contain two bilinear terms (Eqs. 4 and 5).

$$N^S_{u,u',\mathrm{CO}} \cdot N^S_{u,u',\mathrm{H_2O}} = K^{WG} \cdot N^S_{u,u',\mathrm{CO_2}} \cdot N^S_{u,u',\mathrm{H_2}} \qquad \forall (u,u') \in U_{WG} \tag{3}$$

$$N^S_{u,u',\mathrm{CO}} \cdot N^S_{u,u',\mathrm{H_2O}} \le K^{WG}_{u''} \cdot N^S_{u,u',\mathrm{CO_2}} \cdot N^S_{u,u',\mathrm{H_2}} + U \cdot (1 - y_{u''}) \qquad \forall (u,u',u'') \in U^T_{WG} \tag{4}$$

$$N^S_{u,u',\mathrm{CO}} \cdot N^S_{u,u',\mathrm{H_2O}} \ge K^{WG}_{u''} \cdot N^S_{u,u',\mathrm{CO_2}} \cdot N^S_{u,u',\mathrm{H_2}} - U \cdot (1 - y_{u''}) \qquad \forall (u,u',u'') \in U^T_{WG} \tag{5}$$

The steam reforming reactions within the auto-thermal reactor, U_{AT}, are shown in Eqs. 6-9 and contain a total of one bilinear term, four trilinear terms, and one quadrilinear term. Through a reformulation that is similar to Eqs. 4 and 5 above, the steam reforming reactions will contain five bilinear terms and one quadrilinear term. The total nonconvex terms arising from chemical equilibrium is 17 bilinear terms and one quadrilinear term.

$$N^S_{u,u',CO} \cdot N^S_{u,u',H_2}{}^3 = K^{SR}_{CH_4} \cdot N^S_{u,u',CH_4} \cdot N^S_{u,u',H_2O} \quad \forall (u,u') \in U_{AT} \tag{6}$$

$$N^S_{u,u',C_2H_2} \cdot N^S_{u,u',H_2O} = K^{SR}_{C_2H_2} \cdot N^S_{u,u',CH_4} \cdot N^S_{u,u',CO} \quad \forall (u,u') \in U_{AT} \tag{7}$$

$$N^S_{u,u',C_2H_4} = K^{SR}_{C_2H_4} \cdot N^S_{u,u',C_2H_2} \cdot N^S_{u,u',H_2} \quad \forall (u,u') \in U_{AT} \tag{8}$$

$$N^S_{u,u',C_2H_6} = K^{SR}_{C_2H_6} \cdot N^S_{u,u',C_2H_6} \cdot N^S_{u,u',H_2} \quad \forall (u,u') \in U_{AT} \tag{9}$$

The investment cost of the final process topology will be calculated as the sum of the investment cost of all representative process units, U_{Inv}, throughout the superstructure. A total of 60 cost curves are needed, each of which is of the form of Eq. 10, where C_u represents the base cost, SB_u represents the base flow rate, S_u represents the working flow rate, and sf_u is the scaling factor.

$$Inv_u = C_u \cdot \left(\frac{S_u}{SB_u} \right)^{sf_u} \qquad \forall u \in U_{Inv} \tag{10}$$

Bilinear Term Underestimation

For the relaxation, each of the bilinear terms ($z=x \cdot y$) is replaced by a piecewise linear underestimation using a logarithmic partitioning scheme (Misener et al., 2011). The x variable is partitioned into N_P segments based on the upper and lower bounds of the variable (Eq. 11). Binary switches, λ_n, are then used to logically activate one of the partitions. Note that the number of binary variables (N_L) increases logarithmically with the number of partitions.

$$a = \frac{x^U - x^L}{N_P} \tag{11}$$

$$x^L + \sum_{n=1}^{N_L} 2^{n-1} \cdot a \cdot \lambda_n \le x \le a + x^L + \sum_{n=1}^{N_L} 2^{n-1} \cdot a \cdot \lambda_n \tag{12}$$

Continuous switches, Δy_n, and slacks, sl_n, are then used to model the y variable over the active partitions, as shown in Eqs. 13-15.

$$\Delta y_n \le (y^U - y^L) \cdot \lambda_n \tag{13}$$

$$\Delta y_n = (y - y^L) - sl_n \tag{14}$$

$$0 \le sl_n \le (y^U - y^L) \cdot (1 - \lambda_n) \tag{15}$$

The logarithmic partitioning scheme can be established for the auxillary variable z using Eqs. 16-19.

$$z \ge x \cdot y^L + x^L \cdot (y - y^L) + \sum_{n=1}^{N_L} a \cdot 2^{n-1} \cdot \Delta y_n \tag{16}$$

$$z \ge x \cdot y^U + (x^L + a) \cdot (y - y^U) + \sum_{n=1}^{N_L} a \cdot 2^{n-1} \cdot (\Delta y_n - (y^U - y^L) \cdot \lambda_n) \tag{17}$$

$$z \le x \cdot y^L + (x^L + a) \cdot (y - y^L) + \sum_{n=1}^{N_L} a \cdot 2^{n-1} \cdot \Delta y_n \tag{18}$$

$$z \le x \cdot y^U + x^L \cdot (y - y^U) + \sum_{n=1}^{N_L} a \cdot 2^{n-1} \cdot (\Delta y_n - (y^U - y^L) \cdot \lambda_n) \tag{19}$$

This methodology was applied to all bilinear terms in the mathematical model using a total of 4 partitions ($N_L = 2$) for the phase equilibrium terms and 8 partitions ($N_L = 3$) for the remaining terms. The quadrilinear term is relaxed using three successive bilinear relaxations.

Concave Cost Function Underestimation

To underestimate the cost functions, a linear partitioning scheme was utilized which introduces special-ordered-set (SOS2) variables, $y_{i,u}$, to define each piece (Misener et al., 2009). For a given ordered set i, the SOS2 variables are 0-1 continuous and are constrained such that only two variables may be active (value greater than zero) and these two variables must be at adjacent elements (i.e., i and $i + 1$).

$$S_u = \sum_i S\text{-}C_{i,u} \cdot y_{i,u} \qquad \forall u \in U_{Inv} \tag{20}$$

$$Inv_u = \sum_i Inv\text{-}C_{i,u} \cdot y_{i,u} \qquad \forall u \in U_{Inv} \tag{21}$$

The cost function in Eq. 10 may be relaxed using a series of coordinates (S-$C_{i,u}$, Inv-$C_{i,u}$) for each function. Given a working flow rate of a unit, Eq. 20 will define the affine piece of the approximation that bounds the flow rate (i.e., $S\text{-}C_{i-1,u} \le S_u \le S\text{-}C_{i,u}$). The values of the SOS2 variables $y_{i-1,u}$ and $y_{i,u}$ will define the investment cost of the unit based on the linear approximation in Eq. 21.

Branch-And-Bound Tree

To solve the process synthesis model, a branch-and-bound global optimization algorithm (Misener et al., 2009; Misener and Floudas, 2010; Misener et al., 2011) is implemented as detailed below. At each node in the tree, a linear relaxation of the model is solved and the node is branched to create two child nodes. The upper bound is then solved and if the solution is less than the current upper bound, the current upper bound is replaced with the solution value. Nodes are eliminated from the tree if the lower bound is within 1% of the current upper bound. Termination of the algorithm is reached if all nodes in the tree have been processed of if 100 CPU hours have passed.

At the root node of the branch-and-bound tree, it is critical to identify tight ranges on the variables that will be

branched on in the tree. Therefore, the initial step of the global optimization routine is to calculate a high-quality upper bound from a local solution of the problem. An optimality-based bounds tightening procedure is then implemented to determine rigorous upper and lower bounds for the set of variables that participate in the nonlinear terms. The cost for liquid fuels production is bounded from above by the calculated upper bound and then an objective function is constructed where the only terms is one of variables of interest. The model is minimized and subsequently maximized to find the lower and upper bounds of the variable.

Branching Strategies

Upon solving a relaxation at a given node, a variable is selected for branching and the value used to construct the two child nodes is determined. Variables used for partitioning the tree will be either (i) the stream flow rate variables or (ii) the split fraction variables because these two variable sets tended to provide better partitioning of the search space. Due to the binary range partitioning implemented for the "x" variables, it was generally found that branching on these variables provided better partitioning than on the "y" variables.

The variable is selected for branching that has the largest discrepancy between the auxillary and original problem variables (Misener and Floudas, 2010). For a given variable x with lower bound x^L and upper bound x^U, and solution value x', the location for branching, x^{br}, was determined using Eq. 22, where $\lambda_C = 0.1$ is a parameter that selects the branch point partially between the halfway point of the variable range and the optimal solution value.

$$x^{br} = \lambda_C \cdot 0.5 \cdot (x^L + x^U) + (1-\lambda_C) \cdot x' \tag{22}$$

Feasibility Based Bounds Tightening

Prior to determining the lower bound at a node, a series of checks can be made on each variable bound ensure that the bound does not conflict with a constraint that exists within the model. For the split fraction variables ($sp_{u,u'}$), the lower bound may be adjusted if one minus the sum of the upper bounds of all other split fraction variables from that unit are greater than the current lower bound (Eq. 23). The upper bound of a split fraction variable may be adjusted if one minus the sum of the lower bounds of the other unit split fraction variables are lower than the current upper bound (Eq. 24).

$$sp^L_{u,u'} = \max\left(sp^L_{u,u'}, 1 - \sum_{(u,u'')\in U_{SS}}^{u''\neq u'} sp^U_{u,u''}\right) \quad \forall (u,u') \in U_{SS} \tag{23}$$

$$sp^U_{u,u'} = \min\left(sp^U_{u,u'}, 1 - \sum_{(u,u'')\in U_{SS}}^{u''\neq u'} sp^L_{u,u''}\right) \quad \forall (u,u') \in U_{SS} \tag{24}$$

Feasibility checks on the stream flow rate variables are enforced using knowledge of the maximum/minimum possible ratio (R^L/R^U) of the molar flow rate of each species to another in the stream (u,u'). The values for the ratios are determined at the root node upon completion of the optimality-based bounds routine. For any species s in the set S_{CE}, the lower bound on the molar flow rate may be adjusted if the product of the lower bound of another species s' and the minimum ratio between the two species is greater than the current lower bound (Eq. 25). Similarly, the upper bound of a flow rate may be adjusted using the upper bound of another species and the maximum ratio (Eq. 26).

$$N^{S-L}_{u,u',s} = \max\left(N^{S-L}_{u,u',s}, R^L_{u,u',s,s'} \cdot N^{S-L}_{u,u',s'}\right) \quad \forall (u,u',s),(u,u',s') \in S_{CE} \tag{25}$$

$$N^{S-U}_{u,u',s} = \min\left(N^{S-L}_{u,u',s}, R^U_{u,u',s,s'} \cdot N^{S-U}_{u,u',s'}\right) \quad \forall (u,u',s),(u,u',s') \in S_{CE} \tag{26}$$

Computational Results – Global Optimization

The proposed global optimization method was used to analyze the two case studies detailed earlier which focused on 50% and 95% conversion of the feedstock carbon to liquid fuels that exhibit a 50% reduction in the greenhouse gas emissions from petroleum-based processes. The original MINLP model contains 15,439 continuous variables, 30 binary variables, 15,636 constraints, 274 bilinear terms, 1 quadrilinear term, and 60 concave power functions. Each relaxation (lower bound) contains 17,232 continuous variables, 169 binary variables, 18,443 constraints, and 108 SOS2 variables.

The results of the global optimization algorithm are shown in Table 2. For each case study, the computational results are shown after completion of the root node and upon termination of the solver. From Table 2, it is evident that a majority of the computational effort at the root node is spent calculating the upper bound (5,944 s/5,628 s) and the bounds tightening (26,829 s/26,794 s) for the 50% and 95% case studies. This is in contrast with the remaining nodes of the branch-and-bound tree where the majority of time (≥80%) is spent calculating the relaxation.

Upon completion of the root node, the optimality gap between the lower and upper bounds is 31.4% for the 50% case study and 21.2% for the 95% case study. Upon termination, this gap is reduced to 8.6% for the 50% case study and 4.7% for the 95% case study due to both an increase in the relaxation through the branch-and-bound tree and a decrease in the upper bound throughout the tree. Several better feasible solutions were found for most of the case studies during the progression of the tree.

Table 2. Computational results for the branch-and-bound global optimization routine.

Branch-and-Bound Tree Information		Case Study	
		50% Conv.	95% Conv.
Root Node	Relaxation	\$9.12	\$22.94
	UB	\$13.29	\$29.12
	Gap	31.4%	21.2%
	t_{UB} (s)	5944	5628
	t_{OB} (s)	26829	26794
	t_R (s)	1156	1478
Termination	LB	\$11.75	\$27.21
	UB	\$12.85	\$28.56
	Gap	8.6%	4.7%
Nodes		302	320
Total CPU Time (s)		360000	360000

Computational Results – Overall Cost of Liquid Fuels

The upper bound value found at termination of the global optimization routine (Table 2) represents the cost of liquid fuels production (in \$/GJ) for each case study. The resulting components of the overall cost combine to provide a BEOP of \$60.45/bbl for the 50% case and \$149.98/bbl for the 95% case. This cost is decomposed in Table 3 to highlight the contributions of the feedstocks, investment, sequestration, and byproducts to the final value. The feedstock cost is distributed over the coal, biomass, and natural gas feedstocks along with butanes that are needed for gasoline upgrading and freshwater that is needed for losses from the cooling tower and wastewater.

The similarities in the upgrading section for both case studies cause the cost for the butane to remain relatively consistent. The freshwater input to the process is minimal when compared to the cost of the remaining feeds. The propane produced from the process is a byproduct of the upgrading section and therefore is relatively consistent across all twelve case studies. For each of the three feedstocks, the contribution to the overall cost decreases with an increase in the carbon conversion rate. This is expected since higher feedstock-carbon conversion implies that a smaller amount of feedstock is needed to produce a similar amount of liquid fuels. Note that though both processes have different feedstock-carbon conversion ratios, the amount of biomass needed relative to natural gas and coal is relatively similar. This is a result of the 50% reduction in greenhouse gases that must be enforced for each plant. It is assumed that all of the liquid fuels will eventually be burned to release CO_2, so the amount of carbon vented from both the CBGTL process and from burning of the fuels relative to the carbon input to the process is very similar. Thus, the amount of carbon input via biomass must remain relatively constant to reflect this constraint.

CO_2 sequestration is not utilized in either case study since the results of the mathematical model show that it is more economical to purchase additional biomass and vent the CO_2 rather than sequester the CO_2 and purchase cheaper, fossil-fuel feedstocks. For the 50% conversion case, the CO_2 that is vented largely comes from generation of the electricity via an air-blown gas turbine. The combination of CO_2 and N_2 in the turbine effluent makes CO_2 capture and sequestration an economically unfavorable alternative to simply venting the CO_2 and using more biomass as a feed. For the 95% conversion case studies, CO_2 sequestration is also not utilized in the final process topology since most of the CO_2 is reacted with H_2 to form CO via the reverse water-gas-shift reaction. This requires the use of electrolyzers which input electricity to produce the necessary H_2, the result of which can be seen as a positive contribution of the electricity to the overall cost. Some of this electricity may be recovered through the use of a gas turbine, but the recovery of CO_2 from the turbine effluent will be limited due to the N_2 present in the gas turbine inlet air.

Table 3. Breakdown of the overall liquid fuels cost (2009 \$/GJ) upon termination of the branch-and-bound solver.

Cost Contribution	Case Study	
	50% Conv.	95% Conv.
Coal	\$3.63	\$1.92
Biomass	\$5.01	\$2.52
Natural Gas	\$1.63	\$0.86
Butane	\$0.51	\$0.62
Water	\$0.02	\$0.03
CO_2 Sequestration	\$0.00	\$0.00
Investment	\$2.88	\$3.54
Electricity	-\$0.33	\$19.67
Propane	-\$0.50	-\$0.61
Total (\$/GJ)	\$12.85	\$28.56
Total (\$/bbl)	\$60.45	\$149.98

The final contribution to the overall cost comes from the investment of the process units. The investment cost of the 50% conversion case is higher than the 95% case even though the working flow rates through the units are generally higher due to increased feedstock use. For lower feedstock-conversion ratios, a significant amount of byproduct electricity (high negative value in Table 3) is generated, which will require higher feedstock inputs and larger working capacities across all units throughout the process topology. As the amount of feedstock-carbon conversion increases, then a smaller amount of the synthesis gas is directed to the gas turbines, resulting in a decrease in the output electricity and the investment cost. However, as the conversion rate increases, a threshold will be reached where the electrolyzer must be used to convert

some of the CO_2 into CO. Due to the high cost of this unit ($1,000/kW), any decrease in investment cost from smaller working flow rates is offset by the investment cost of the electrolyzer. This fact is evident in the 95% case since the total investment cost is higher than the 50% case. Note that if the electrolzyer investment cost was reduced, the 95% conversion case would likely have a lower overall investment cost.

Supply Chain Optimization

Based on the process synthesis results for the design of the stand-alone CBGTL plant, we investigated the feasibility of the CBGTL process to fulfill the entire United States transportation fuel demands in an energy supply chain optimization problem. The advantage of a hybrid energy process such as the CBGTL process is that the United States can utilize domestically available resources, namely sustainably harvested biomass residues, coal, and natural gas to produce gasoline, diesel, and kerosene. Further, the incorporation of different types of biomass as feedstock helps mitigate the greenhouse gas emissions for the transportation sector and drive the shift towards renewable energy production. As the hybrid CBGTL process involves multiple energy resources and economic domains, an integrated and systematic approach that evaluates the interconnection between key stakeholders is crucial to attain efficient resource allocation and a cost-competitive energy supply chain.

To this effect, we developed an optimization framework to solve a large-scale, nationwide energy supply chain problem that takes into account the varying degrees of resource availabilities and the demand profile for the United States. The supply chain begins at the feedstock source locations, ends at the demand locations, and consists of optimized CBGTL facilities using the process synthesis with simultaneous heat and power integration method. Note that the CBGTL plant designs used in the supply chain problem corresponds to the local solutions of the process synthesis optimization model.

Feedstock Availabilities

The CBGTL process is designed to process only one type of biomass, coal, and natural gas to produce fuels. However, to replace all petroleum-based transportation fuels using the CBGTL process, the United States would have to utilize multiple different types of coal, biomass, and natural gas feedstocks available within the country. For the supply chain optimization problem, we have selected six different types of coal, three representative biomass feedstock types, and one natural gas composition. The six coal types (i.e., lignite, sub-bituminous, high-, medium-, and low-volatile (HV, MV, LV) bituminous, and anthracite coal) represent the available coal sources in the United States, and biomass is categorized into three representative groups, namely the forest residues, agricultural residues, and perennial grasses (Elia et al., 2011). One generic composition for natural gas is assumed based on an average composition of wellhead production in the United States (NETL, 2004). The availabilities of all feedstocks are obtained from government-based databases and are analyzed based on assumptions in Elia et al., 2011. The feedstock parameters, which include (i) the location of feedstock resources, (ii) the amount available for the CBGTL process that does not interrupt with current usage of feedstock, and (iii) the purchase costs from each location, are inputs to the supply chain optimization model.

Optimized CBGTL Facilities

For each coal, biomass, and natural gas feedstock combination, the CBGTL plant design is optimized via the aforementioned process synthesis approach. Additionally, three plant capacities are considered, namely the 10,000 barrels per day (BPD; small), 50,000 BPD (medium), and 200,000 BPD (large) fuel producing plants, and two CO2 management alternatives are included, namely plant designs with and without sequestration systems.

To fulfill the 50% reduction of greenhouse gas (GHG) emissions target by 2050, agreed by international leaders at the G8 Summit, the process synthesis optimization model directly accounts for the life cycle emissions calculation to determine the proportions of the feedstocks. The well-to-wheel analysis starts from the GHG emitted during feedstock acquisition, feedstock transportation, the CBGTL process, and fuel product delivery. Biomass provides a negative balance to the emissions figure and can be used to achieve the emissions target. To comply with the 50% reduction from petroleum-based processes (i.e., 91.6 kg CO_2 equivalent/GJ lower heating value (LHV) of fuels produced (Larson et al., 2010)), only a limited amount of CO_2 from the CBGTL plant can be emitted to the atmosphere, and the rest is channeled in one of two options: i) sequester CO_2 sequestration or ii) CO_2 recycle back into the CBGTL process.

The distinct combinations of six coal feedstock types, three biomass feedstock types, one natural gas composition, three plant capacities, and two carbon management options give rise to 108 optimal plant topologies (i.e., 6 x 3 x 1 x 3 x 2 = 108) and the process synthesis results form the basis of the plant parameter inputs for the optimization model. These plant parameters include (i) feedstock flow rate requirements, ii) electricity requirement, iii) amount of CO_2 sequestered, and iv) the levelized investment costs that include capital investment, operational, and utilities costs. The energy supply chain optimization model can select one out of the 108 plant topologies for each candidate location and its corresponding parameters for that location.

Candidate Facility Locations

A superset of candidate facility locations throughout the United States is postulated and input to the optimization model. This section outlines the methodologies used to generate this superset of locations.

Initially, every United States county centroid is postulated to be a potential plant location, adding to 3136 locations excluding Hawaii. This list is subsequently reduced by applying elimination criteria to filter out locations that are deemed unsuitable.

A set of connections that consist of linkages between feedstock counties, modes of transportation, and facility locations is defined. In the supply chain, coal is delivered by rail, biomass by truck, and natural gas by interstate and intrastate pipelines. For each of the linkage, a transportation cost is calculated. Then, a maximum transportation cost for each feedstock type is imposed such that any linkage that incurs costs above this maximum cost is taken out of the set. In imposing these criteria, we allowed coal and natural gas transportation to travel greater distances than biomass transportation.

Based on the remaining linkages, we defined sets of counties that can receive biomass, coal, and natural gas within the cost criteria, amounting to 3136, 2866, and 2493 counties, respectively. A valid candidate of facility location for the energy supply chain, however, must be able to receive all three feedstock inputs within the imposed criteria. Thus, the overlap between the three sets of counties yielded a total of 1880 valid candidate locations.

All 1880 counties then are ranked separately based on the amount of coal, biomass, and natural gas produced in each county. Thus, each county is associated with three ranking values associated with each feedstock, and a final rank order list is constructed based on the combined coal, biomass, and natural gas rankings. Based on this rank order list, we can select the top N number of counties for each state that can serve as a potential CBGTL facility site. A parametric analysis was completed to determine what N should be, taking the top 10-100% of the 1880 potential sites in 10% increment (e.g., if 10% is considered, we take the ceiling of the 10% of the total potential sites on a per state basis). Trade-offs between the improved value of the objective function, increased computational time, and model complexity with the increased number of candidate locations were examined and it was determined that the top 70% sites on a per state basis gave the best results. The final reduced set is comprised of 1329 candidate locations for the CBGTL supply chain network.

Energy Supply Chain Mathematical Model

The CBGTL facilities and the candidate locations, along with information on the nationwide configuration for the feedstock, the United States transportation fuel demands, and modes of transportation obtained from published government-based databases, serve as parameter inputs to the energy supply chain optimization model. The energy supply chain optimization problem is formulated as a large-scale MILP model, representing the discrete and continuous decisions in the supply chain, and solved using CPLEX to give the optimal topology of the CBGTL supply chain at the minimum overall cost of fuel production for the entire network. The solution will include i) the location of CBGTL facilities, ii) the specific types and capacities of the selected facilities, iii) the complete supply chain topology from the feedstock sources to the demand locations with the flow rate amounts of each interconnection, and iv) the costs associated with each segment of the supply chain problem.

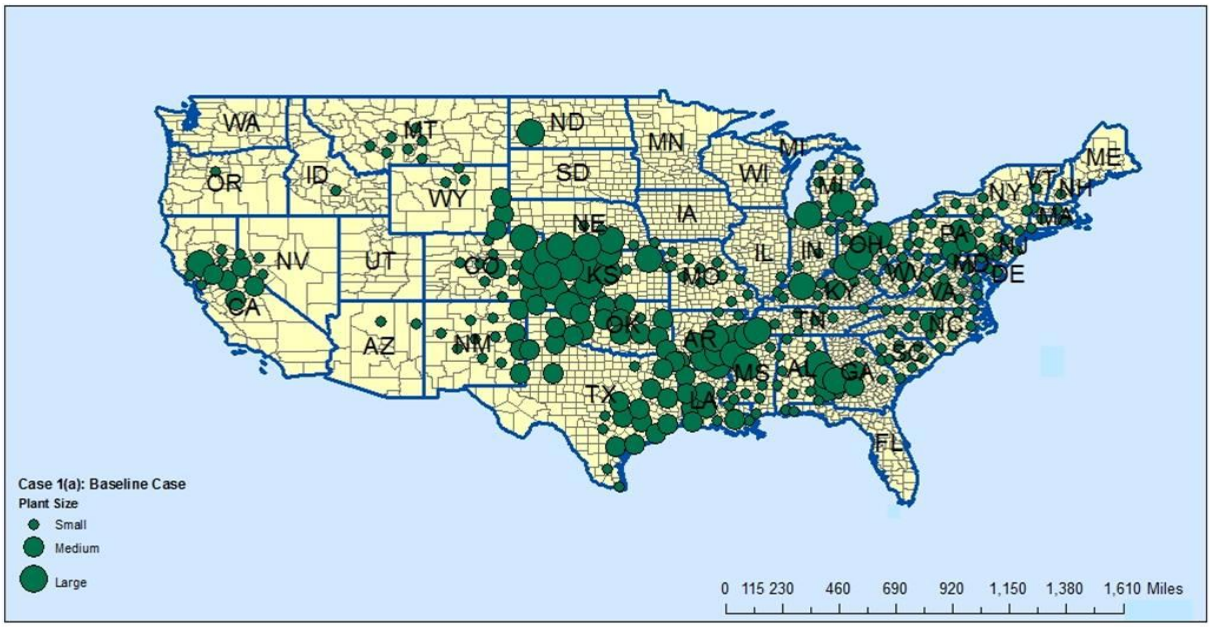

Figure 2. Graphical representation of the locations of selected facilities in case study (1a). The facilities are represented by green circles centered at the proposed facility location with corresponding sizes

Computational Studies

The supply chain optimization model is solved to give the optimal CBGTL plant network for the United States. Facets of the model solution provide a quantitative basis to evaluate and examine trade-offs in investment and planning decisions. A total of 300 facilities are selected, consisting of 199 small, 60 medium, and 41 large facilities and producing 15.1%, 22.7%, and 62.2% of the total fuel demand, respectively. Of the 300 total facilities, 275 of them include a carbon sequestration system (199 small, 57 medium, and 19 large) and the remaining 25 are facilities have no sequestration system (3 medium, and 22 large), which are mostly located in the southeast and central regions of the United States.

Fuel production favors large facilities due to economies of scale. Figure 2 is the graphical representation of the network layout, which shows notable clusters of large facilities located in the central, midwest, and southeast regions. Texas has the highest number of selected facilities, although the highest level of fuel production takes place in Kansas, which produces 16.9% of the total fuels, followed by Arkansas (9.3%), Colorado (7.0%), Texas (6.8%), and Ohio (6.4%). Kansas has 11 large and 3 small facilities, while Arkansas has 5 large facilities, and Colorado and Ohio with 4 large facilities each. The more abundant biomass resources allow the selection of large-sized facilities in the central, midwest, and southeast regions. Texas, which has a more distributed profile of biomass resources, has small and medium plants. Additionally, fuel production in the eastern part of the country also favors small facilities with a few medium facilities in Pennsylvania, West Virginia, Virginia, and North Carolina where coal sources are relatively close.

The medium non-sequestration facilities are located in Georgia (2 facilities) and Louisiana (1), and the large non-sequestration facilities are in Alabama (3), Arkansas (5), California (1), Colorado (4), Georgia (1), Kansas (3), Mississippi (3), Oklahoma (1), and Tennessee (1). Plants without sequestration systems are distinct from their counterpart due to their high electricity requirements for the on-site hydrogen production via an electrolyzer unit and their reduction of feedstock requirements due to the carbon recycle in the system. Plants with sequestration generally produce a small amount of electricity that can be sold to the grid.

The overall break even oil price for the entire network is calculated to be $87.46/bbl crude oil. The network favors fuel production in large facilities due to economies of scale. A total of 8,200,000 BPD of fuels is produced in large facilities, 3,000,000 BPD in medium facilities, and 1,990,000 BPD in small facilities. The highest contributing factors in the overall cost are the total investment costs for installing all CBGTL plants, the cost of electricity, and the biomass purchase cost for the network.

This overall cost of fuel production, however, varies from state to state, and the initial developments of the CBGTL network will naturally gravitate towards areas where fuels can be produced at a lower cost. The lowest costs of fuel production are achieved in Michigan ($41.41/bbl), Ohio ($42.21/bbl), and Kentucky ($43.01/bbl), generally located in the midwest region where biomass is abundant and coal and natural gas are nearby. Kansas, where the highest level of fuel production takes place, averages at $77.32/bbl. The highest costs are in Georgia ($133.79/bbl), Colorado ($131.40/bbl), Alabama ($130.03/bbl), Arkansas ($127.75/bbl), and Mississippi ($125.24/bbl). These states are generally in the southeastern region of the United States, where non-sequestration plants are selected.

Coal, biomass, and natural gas distributions from their source locations to the CBGTL facilities, and the product distributions from the facilities to the demand locations are analyzed by dividing the United States in several regions, namely the northeast, southeast, Midwest, central, southwest, and Western regions. A regional profile in the distribution of feedstock and products in the network emerges from the model solution, where most of the commodities are allocated within their initial regions. This feature is most evident in the biomass distribution firstly, biomass is more distributed in production, allowing short-distance delivery. In contrast, coal and natural gas are produced in a large-scale, centralized manner, thus inter-region delivery is often required. Secondly, biomass transportation cost is relatively higher compared to coal and natural gas on a per energy basis, favoring further the short-distance transportation.

Total electricity requirement for the network equals to 183.4 GW, largely due to the electricity consumption of no-sequestration plants. This amount is about 18% of current United States net electricity generation capacity, which is reported to be 1025.4 GW in the summer and 1063.8 GW in the winter for the year 2009 (EIA, 2010). The total biomass usage amounts to 618.40 million dry tonnes/yr, which requires expansion of sustainable biomass production, currently estimated to be 460 million dry tones/yr. This value, however, is projected to reach 1 billion dry tones in the future (DOE and USDA, 2005). Coal usage (923.96 million short tons/yr) also compares to the United States production and consumption data, reported to be 1072.8 and 1000.4 million short tons in 2009, respectively (EIA, 2010). Finally, natural gas usage for the network (5,28 billion cubic feet) is much below current dry gas production, taken to be 20,580 billion cubic feet in 2009 (EIA, 2010).

Well-to-wheel GHG emissions for the entire network are calculated via a life cycle analysis and the overall average emissions equals to 45.81 kg CO_2/GJ, 50% less from petroleum emissions is achieved for all case studies and demonstrating that the 2050 target is achievable in the near future. From the overall analysis of the energy supply chain, results suggest that the CBGTL supply chain has potential to satisfy the United States transportation fuel

demands with domestically available resources with significant environmental gains.

Conclusions

Hybrid feedstock energy processes show potentials in fulfilling transportation fuel demands and alleviating greenhouse gases emissions. A hybrid CBGTL superstructure that converts biomass, coal, and natural gas into gasoline, diesel, and kerosene with near 100% carbon conversion is developed and optimized via solving a large-scale MINLP problem with simultaneous heat, power, and water integration. Global optimization approaches are employed using piecewise linear underestimators for the nonconvex terms in the model to obtain optimal CBGTL plant topologies. A MILP model is subsequently formulated to determine the optimal CBGTL supply chain network that gives the minimum overall cost of producing transportation fuels to fulfill United States demand. Results suggest that the CBGTL network is economically competitive with petroleum based processes, with additional benefits of significant GHG emissions reduction.

Acknowledgments

The authors acknowledge partial financial support from the National Science Foundation (NSF EFRI-0937706).

References

Agrawal, R., Singh, N. R., Ribeiro, F. H., Delgass, W. N. (2007). Sustainable fuel for the transportation sector. *PNAS*, 104, 4828.

Baliban, R. C., Elia, J. A., Floudas, C. A. (2010). Toward Novel Biomass, Coal, and Natural Gas Processes for Satisfying Current Transportation Fuel Demands, 1: Process Alternatives, Gasification Modeling, Process Simulation, and Economic Analysis. *Ind. Eng. Chem. Res.*, 49, 7343.

Baliban, R. C., Elia, J. A., Floudas, C. A. (2011). Optimization Framework for the Simultaneous Process Synthesis, Heat and Power Integration of a Thermochemical Hybrid Biomass, Coal, and Natural Gas Facility. *Comp. Chem. Eng.*, 35, 1647.

Bechtel. (1998). Aspen Process Flowsheet Simulation Model of a Battelle Biomass-Based Gasification, Fischer-Tropsch Liquefaction and Combined-Cycle Power Plant, Contract No. DE-AC22-93PC91029.

DOE, USDA. (2005). Biomass as feedstock for a bioenergy and bioproducts industry: The technical feasibility of a billion-ton annual supply.

EIA. (2010). Annual Energy Outlook 2010.

Elia, J. A., Baliban, R. C., Floudas, C. A. (2010). Toward Novel Biomass, Coal, and Natural Gas Processes for Satisfying Current Transportation Fuel Demands, 2: Simultaneous Heat and Power Integration. *Ind. Eng. Chem. Res.*, 49, 7371.

Elia, J. A., Baliban, R. C., Xiao, X., Floudas, C. A. (2011). Optimal Energy Supply Network Determination and Life Cycle Analysis for Hybrid Coal, Biomass, and Natural Gas to Liquid (CBGTL) Plants Using Carbon-based Hydrogen Production. *Comp. Chem. Eng.*, 35, 1399.

Larson, E. D., Jin, H., Celik, F. E. (2009). Large-scale gasification-based coproduction of fuels and electricity from switchgrass. *Biofuels Bioprod. Bioref.,* 3, 174.

Larson, E. D., Fiorese, G., Liu, G., Williams, R. H., Kreutz, T. G., Consonni, S. (2010). Co-production of decarbonized synfuels and electricity from coal+biomass with CO2 capture and storage: An Illinois case study. *Energy Environ. Sci.,* 3, 28.

Misener, R., Gounaris, C. E., Floudas, C. A. (2009) Global Optimization of Gas Lifting Operations: A Comparative Study of Piecewise Linear Formulations. *Ind. Eng. Chem. Res.*, 48, 6098.

Misener, R. and Floudas, C. A. (2010). Global Optimization of Large-Scale Generalized Pooling Problems: Quadratically Constrained MINLP Models. *Ind. Eng. Chem. Res.*, 49, 5424.

Misener, R., Thompson, J. P., Floudas, C. A. (2011). APOGEE: Global optimization of standard, generalized, and extended pooling problems via linear and logarithmic partitioning schemes. *Oper. Res.*, 35, 876.

NETL. (2004). Quality Guidelines for Energy System Studies.

Kreutz, T. G., Larson, E. D., Liu, G., Williams, R. H. (2008). Fischer-Tropsch Fuels from Coal and Biomass. *Proc. 25th Int. Coal Con.*

National Research Council. (2009). Liquid Transportation Fuels from Coal and Biomass: Technological Status, Costs, and Environmental Issues. *Nat. Acad. Press.*

Vliet, O., Faaij, A., Turkenburg, W. (2009). Fischer-Tropsch diesel production in a well-to-wheel perspective: A carbon, energy flow and cost analysis. *Ener. Con. Manage.,* 50, 855.